CEAS-GNC-2022-041

CEAS EuroGNC 2022
"Conference on Guidance, Navigation and Control"
3-5 May 2022 @ Technische Universität Berlin, Germany

Impact Angle Control with Generalized-Polynomial Look-Angle Formulation

Shen Kang Engineer, China Academy of Launch Vehicle Technology, 100076, Beijing, China. shenkang90@sina.com

Raziye Tekin Senior Lead Engineer, Roketsan Inc., 06780, Ankara, Turkey. razytekin@gmail.com

Lei Zhang Engineer, China Academy of Launch Vehicle Technology, 100076, Beijing, China. leizhang_calt@sina.com

ABSTRACT

In this paper, the missile guidance problem with desired impact angle is investigated based on a generalized-polynomial look-angle formulation. Shaped by a time dependent polynomial of arbitrary order, the look angle profile is given by a set of boundary constraints while one coefficient in the polynomial is preserved as the guidance gain. Since the impact angle problem in nonlinear domain is a challenging task, linearized engagement geometry is employed to establish the impact angle constraint, which determines the guidance gain. With the help of frame convention, the guidance gain is further updated continuously to perform in the nonlinear domain which leads to a closed-loop form of the guidance law. Moreover, a method to satisfy the look-angle constraint during the flight is proposed. Simulated cases are provided to demonstrate the effectiveness and robustness of the proposed guidance law.

Keywords: Impact angle control; Polynomial shaping guidance; Look-angle shaping; Field-of-view Constraint

1 Introduction

Missile guidance problem has evolved into trajectory shaping problem within the increased demands not only to hit the target directly but also with extra conditions. These extra demands depending on the application might be impact time, impact angle or both simultaneously, in which the impact angle control has been the most popular among all. One of the main reasons of impact angle's popularity is because when the impact angle is controlled, it is possible to increase the warhead effectiveness or hit the target from the weak points, reducing collateral damage, all of which are very much related to the efficiency of the hit.

The history of impact angle control dates back nearly fifty years in Ref. [1]. When the solutions of impact angle control problem are analyzed, it is possible to observe that there are several design frameworks being used. One of these frameworks uses the proportional navigation with modifications such as adding a bias or using in a switched design structure. Several examples of biased PN guidance for impact angle control are given in Ref. [2-6]. In Erer et al. and Kim et al., the bias is added to the PN guidance command for the first phase of the engagement. In Ref. [4], the bias is designed as an exponential decaying error function in a continuous form rather than their previous switched structured

solution. Ref. [5] presents a two-phased PN guidance for impact angle control, where the switching instant designed to satisfy the final constraint. Ref. [6] shows that the using PN based method, it is also possible to control the impact angle without switching strategy. Second, the framework of optimal control and sliding mode control also constitutes an appropriate basis for the solution as exemplified in Ref. [7-9]. In Ref. [7], optimal control is used along with a time-to-go estimation method for impact angle problem. The state-dependent Riccati equation-based control law given is obtained as a function of both the range-to-go and the time-to-go in Ref. [8]. Again, a sliding-mode separated guidance and control approach is formulated in Ref. [9] where the guidance command has two components for reaching and remaining on the sliding surface. Ref. [10] also provides another example of the sliding mode control used for impact angle considering finite time convergence and avoiding singularity in the guidance command. Lastly, trajectory shaping using the time-dependent polynomials as a design framework shall be mentioned. Ref. [11] and Ref. [12] solve the impact angle problem using polynomials for stationary targets. Moreover, Ref. [13] designs a polynomial for line of sight angle in terms of range-to-go and the coefficients of the polynomial are found with respect to the initial and the final conditions.

As the second important topic to mention in addition to the design frameworks is the guidance law design under constraints. Since the physical systems have a limit such as acceleration capability or look angle, these constraints also need to be considered during the guidance algorithms design. In this respect, Ref. [11] considers acceleration constraint and Ref. [14] is interested in look-angle constraint within PN based design. Ref. [15] is an example of impact angle control using the framework of polynomials and handling with the look-angle constraint. In Ref. [16], look-angle constraint is under scope within the framework of sliding mode control. In Ref. [17], the look-angle and the acceleration constraints using the PN in a switched structure are considered simultaneously.

In this study, impact angle is controlled via using polynomials for stationary targets. Apart from the current literature, here a different shaping function and a shaping parameter is being used for the first time for impact angle control problem, motivating from the introduced new framework for impact time control as given in Ref. [18]. Ref. [11] shapes the acceleration in terms of time-to-go and in Ref. [12], attitude is described as a cubic polynomial of downrange. As given in Ref. [13], line-of-sight is shaped with respect to relative range. To the knowledge of the authors, impact angle control is not designed shaping the look angle. Furthermore, the shaping function is neither range nor time-to-go, but time itself. Additionally, the shaping function can be written for any order of the polynomials not limited to one order. Thus, adjusting the order of the polynomial, the guidance law attains two critical abilities besides hitting the target from a desired direction. Such that, it performs as good as the OGL proposed in Ref. [19] on the total control effort, which is optimal in the linear domain. Besides, it poses boundary conditions on the derivatives of the look angle, which leads to a zero-terminal acceleration. Moreover, the structure of the proposed guidance law provides a solution under look-angle constraint.

In section 2, the engagement kinematics are given against a stationary target. Section 3 is for presenting the look-angle shaping method. Providing the initial and final boundaries, the guidance command and the coefficients of the polynomial are found. Then, the solutions for the guidance gain determination is given in section 4. Here, first linearized domain solution is given and the closed form guidance law is introduced. Afterwards, modification for the nonlinear kinematics is presented. In section 5, a different methodology benefiting from the guidance command structure and time-to-go calculation is suggested for impact angle control under look-angle constraint. Lastly in section 6,

simulation studies are given to show and compare the efficiency of the method, in which different cases are discussed.

2 Engagement Kinematics

The engagement geometry between a missile *M* and a stationary target *T* is depicted in Figure 1, where the range between the objects is *r*. The flight path angle, the line-of-sight (LOS) angle and the look angle are respectively denoted by γ, λ and ε, which are positive in the counter clockwise direction. The velocity of the missile is *V* and the acceleration, $a = V\dot{\gamma}$, is used to change the direction of the velocity. The equations of relative motion are described in differential form:

$$\dot{r} = -V\cos\varepsilon \tag{1}$$

$$\dot{\varepsilon} = V\frac{\sin\varepsilon}{r} + \dot{\gamma} \tag{2}$$

and the following equation is validated by the geometric relationship:

$$\gamma = \varepsilon + \lambda \tag{3}$$

In this study, the guidance command that achieves the desired impact angle γ_d as well as zero miss distance, i.e. $r = 0$, is investigated via shaping the look-angle profile using a generalized time dependent polynomial.

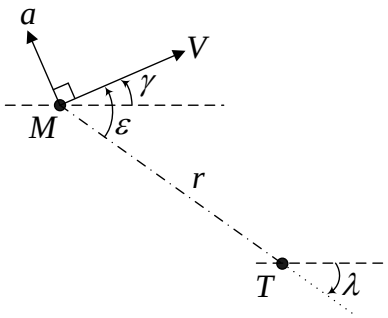

Fig. 1 Engagement geometry

3 Guidance Command Derivation for Impact Angle Control

It is easy to find out from the time derivative of equation (3) that the guidance command consists of two parts in nature:

$$\dot{\gamma} = \dot{\varepsilon} + \dot{\lambda} \tag{4}$$

Since $\dot{\lambda}$ can be attained using on-board sensors, the problem encountered herein is to determine a proper satisfying the terminal conditions for both the collision and the desired impact angle.

To this end, consider the look-angle profile as an *n*-th order polynomial in terms of time

$$\varepsilon = \kappa_n t^n + \kappa_{n-1} t^{n-1} + ... + \kappa_2 t^2 + \kappa_1 t + \kappa_0 \tag{5}$$

where *n* is an integer and $\kappa_0, \kappa_1, \ldots, \kappa_{n-1}, \kappa_n$ are the coefficients to be determined with respect to boundary conditions indicating the desired engagement geometry. If one coefficient is designated to fulfill the impact angle condition, i.e., the coefficient of the highest order term, there would be n

coefficients left undetermined in equation (5). In order to define the polynomial properly, *n* independent constraints are to be found. Therefore, the boundary conditions of the look angle and its derivatives, which can be explicitly established on the base of equation (5), are employed to directly constrain the polynomial.

Firstly, the initial condition of the look angle is given as

$$\varepsilon(0) = \varepsilon_i \tag{6}$$

where ε_i denotes the initial look angle. Owing to the fact that leads to zero miss distance, the terminal condition of the look angle is as follows

$$\varepsilon(t_f) = \kappa_n t_f^n + \kappa_{n-1} t_f^{n-1} + ... + \kappa_2 t_f^2 + \kappa_1 t_f + \kappa_0 = 0 \tag{7}$$

where t_f is assumed to be the time instant exactly when the missile hits the target. It can be seen that at least three coefficients are occupied to stay in accordance with the initial condition and ensure the collision as well as the desired impact angle, indicating $n \geq 2$ for the order of the polynomial.

In the case for $n > 2$, it is noticed that $n-2$ more conditions are still required to provide enough constraints on equation (5) thus it can be properly defined. Therefore, the terminal conditions exerted on the time derivatives of the look angle are included as

$$\begin{bmatrix} \dfrac{\mathrm{d}\varepsilon}{\mathrm{d}t} \\ \dfrac{\mathrm{d}^2\varepsilon}{\mathrm{d}t^2} \\ \dfrac{\mathrm{d}^3\varepsilon}{\mathrm{d}t^3} \\ \vdots \\ \dfrac{\mathrm{d}^{n-2}\varepsilon}{\mathrm{d}t^{n-2}} \end{bmatrix}_{t=t_f} = \begin{bmatrix} n\kappa_n t_f^{n-1} + (n-1)\kappa_{n-1} t_f^{n-2} + \ldots + 3\kappa_3 t_f^2 + 2\kappa_2 t_f + \kappa_1 \\ n(n-1)\kappa_n t_f^{n-2} + (n-1)(n-2)\kappa_{n-1} t_f^{n-3} + \ldots + 6\kappa_3 t_f + 2\kappa_2 \\ n(n-1)(n-2)\kappa_n t_f^{n-3} + (n-1)(n-2)(n-3)\kappa_{n-1} t_f^{n-4} + \ldots + 6\kappa_3 \\ \vdots \\ \dfrac{n!}{2}\kappa_n t_f^2 + (n-1)!\kappa_{n-1} t_f + (n-2)!\kappa_{n-2} \end{bmatrix} = \bar{0} \tag{8}$$

where $\bar{0}$ denotes an $(n-2)\times 1$ vector.

It is obvious that equations (6-8) define *n* boundary conditions while there are *n+1* coefficients unknown in equation(5), so κ_n can be used to express the other coefficients according to the boundary conditions. Firstly, equation (6) leads to an evident result independent of *n*:

$$\kappa_0 = \varepsilon_i \tag{9}$$

Furthermore, with equations (7) and (8) involved, the solving process would vary regarding the choice of *n*, so here several examples are taken for characterization. For *n* = 2, 3 and 4, the corresponding results showing the relation between the polynomial order, the boundary conditions and the coefficients are listed in Table 1. As seen, the boundary conditions are proper to present all coefficients of the polynomial in terms of κ_n.

Table 1 Coefficients with different polynomial order

Shaping function	Boundary conditions	Coefficients in terms of κ_n
$\varepsilon = \kappa_2 t^2 + \kappa_1 t + \kappa_0$	$f_1 : \varepsilon(0) = \kappa_0 = \varepsilon_i$ $f_2 : \varepsilon(t_f) = \kappa_2 t_f^2 + \kappa_1 t_f + \kappa_0 = 0$	$\kappa_1 = -\left(\kappa_2 t_f + \frac{\varepsilon_0}{t_f}\right)$
$\varepsilon_3 = \kappa_3 t^3 + \kappa_2 t^2 + \kappa_1 t + \kappa_0$	$f_1 : \varepsilon(0) = \kappa_0 = \varepsilon_i$ $f_2 : \varepsilon(t_f) = \kappa_3 t_f^3 + \kappa_2 t_f^2 + \kappa_1 t_f + \kappa_0 = 0$ $f_3 : \dot{\varepsilon}(t_f) = 3\kappa_3 t_f^2 + 2\kappa_2 t_f + \kappa_1 = 0$	$\kappa_1 = \kappa_3 t_f^2 - \frac{2\varepsilon_0}{t_f}$ $\kappa_2 = -\left(2\kappa_3 t_f - \frac{\varepsilon_0}{t_f^2}\right)$
$\varepsilon_4 = \kappa_4 t^4 + \kappa_3 t^3 + \kappa_2 t^2 + \kappa_1 t + \kappa_0$	$f_1 : \varepsilon(0) = \kappa_0 = \varepsilon_i$ $f_2 : \varepsilon(t_f) = \kappa_4 t_f^4 + \kappa_3 t_f^3 + \kappa_2 t_f^2 + \kappa_1 t_f + \kappa_0 = 0$ $f_3 : \dot{\varepsilon}(t_f) = 4\kappa_4 t_f^3 + 3\kappa_3 t_f^2 + 2\kappa_2 t_f + \kappa_1 = 0$ $f_4 : \ddot{\varepsilon}(t_f) = 12\kappa_4 t_f^2 + 6\kappa_3 t_f + 2\kappa_2 = 0$	$\kappa_1 = -\left(\kappa_4 t_f^3 + \frac{3\varepsilon_i}{t_f}\right)$ $\kappa_2 = 3\kappa_4 t_f^2 - \frac{3\varepsilon_i}{t_f^2}$ $\kappa_3 = -\left(3\kappa_4 t_f + \frac{\varepsilon_i}{t_f^3}\right)$

However, since equation (4) indicates that $\dot{\varepsilon}$ is the key point to generate the guidance command, hence instead of having all the coefficients described by κ_n, the coefficients related to the look-angle rate are the only ones that matter. The close-form of the time derivative of equation (5) is obtained by letting $t \to 0$ and $t_f \to t_f - t$:

$$\dot{\varepsilon} = \kappa_1 \tag{10}$$

Using equation (10), it is possible to present the closed-form look-angle rate and the results for *n* = 2, 3 and 4 can be concluded from the third column of Table 1:

$$\dot{\varepsilon}_2 = -\kappa_2 (t_f - t) - \frac{\varepsilon}{(t_f - t)} \tag{11}$$

$$\dot{\varepsilon}_3 = \kappa_3 (t_f - t)^2 - \frac{2\varepsilon}{t_f - t} \tag{12}$$

$$\dot{\varepsilon}_4 = -\kappa_4 (t_f - t)^3 - \frac{3\varepsilon}{t_f - t} \tag{13}$$

where κ_n appears to be the only element to be designed accordingly. By mathematical induction, equations (11-13) can be generalized for arbitrary *n*:

$$\dot{\varepsilon} = (-1)^{n-1} \kappa_n (t_f - t)^{n-1} - \frac{n-1}{t_f - t} \varepsilon \tag{14}$$

Then the guidance command can be obtained by the aid of equation (4):

$$\dot{\gamma} = (-1)^{n-1} \kappa_n (t_f - t)^{n-1} - \frac{n-1}{t_f - t} \varepsilon + \dot{\lambda} \tag{15}$$

where κ_n can be seen as the guidance gain and $t_f - t$ plays as the time-to-go which can be estimated in flight.

Besides, by integrating equation (14) on the time interval $\left[0,t_f\right]$, the generalized look-angle profile in terms of κ_n can be also obtained:

$$\varepsilon(t)=\left(t-t_f\right)^{n-1}\left(\frac{\varepsilon_i}{(-1)^{n-1}t_f^{n-1}}+\kappa_n t\right) \tag{16}$$

4 Guidance Gain Determination for Impact Angle Control

In this section, the connection between the guidance gain and the desired impact angle is established to define completely the polynomial so the guidance command. Solving the guidance gain in the nonlinear domain to reveal the impact angle requires numerical integration performed on equations (1) and (2), which shall be preferably avoided due to the burdened computation process. Therefore, the guidance gain in the linear domain is provided analytically in this section. Afterwards, the guidance gain for the nonlinear domain is obtained via continuously updating the linear one with respect to the current engagement geometry.

4.1 Linear Impact Angle Control

The linearized engagement is assumed where the horizontal component of the velocity is constant, and the missile is allowed to perform corrective maneuvers only in the vertical direction. Denoting y as the vertical displacement of the missile, then the path and LOS angles are represented as $\gamma=\dot{y}/V$ and $\lambda=-y/V(t_f-t)$, respectively. Using equation (4), the LOS rate also can be revealed as $\dot{\lambda}=-\varepsilon/\left(t_f-t\right)$. With the linear domain definitions, the following differential equation is established to bridge y and ε:

$$\dot{y}+\frac{y}{t_f-t}=V\varepsilon \tag{17}$$

Combining with equation (16), the solution of equation (17) is given

$$y(t)=C(t-t_f)+V(t-t_f)^n\left(\frac{\varepsilon_i}{\left(n-1\right)(-1)^{n-1}t_f^{n-1}}+\kappa_n\frac{t_f+\left(n-1\right)t}{n(n-1)}\right) \tag{18}$$

where C is the integration constant found via the initial conditions:

$$C=-\left(\frac{y_i}{t_f}+\frac{V\varepsilon_i}{n-1}+(-1)^{n-1}\kappa_n\frac{Vt_f^n}{n(n-1)}\right) \tag{19}$$

Here, y_i is the initial displacement.

Since the linearized flight path angle is also available, resulting from the vertical displacement, the impact angle can be revealed by the time derivative of equation (18) at $t=t_f$:

$$\gamma\left(t_f\right)=-\left(\frac{y_i}{t_f}+\frac{\varepsilon_i}{n-1}+(-1)^{N-1}\kappa_n\frac{t_f^n}{n(n-1)}\right) \tag{20}$$

Let $\gamma\left(t_f\right)=\gamma_d$ and the guidance gain that satisfies the desired impact angle is obtained:

$$\kappa_n = \frac{n(n-1)\left(\gamma_d + \dfrac{y_i}{t_f} + \dfrac{\varepsilon_i}{n-1}\right)}{(-1)^n t_f^n} \tag{21}$$

Thus, equation (21) provides the last piece in equation (15) and completes the guidance command generation in the linear domain.

4.2 Nonlinear Impact Angle Control

It can be observed that initial conditions such as y_i and ε_i are required in the guidance gain calculation, and the guidance gain remains constant during the engagement, which may induce linearized error due to that the derivation in the linear domain assumes that ε is always small enough. In order to prevent the guidance law from the aforementioned drawbacks, a method to update the guidance gain in the nonlinear domain according to the current LOS is presented in this subsection.

Frame convention is employed to recognize the engagement geometry in the current LOS frame, which leads to $y_i \to 0$ and $\varepsilon_i \to 0$. The desired impact angle described in the inertial frame is also transformed with respect to the current LOS, i.e. $\hat{\gamma}_d = \gamma_d - \lambda$. Moreover, the impact time is updated by time-to-go, i.e. $t_f \to t_f - t = t_{go}$. Implementing these modifications yields the guidance gain as

$$\kappa_n = \frac{n(n-1)\hat{\gamma}_d + n\varepsilon}{(-1)^n t_{go}^n} \tag{22}$$

and the guidance command given as

$$\dot{\gamma} = (-1)^{n-1}\kappa_n t_{go}^{n-1} - \frac{n-1}{t_{go}}\varepsilon + \dot{\lambda} \tag{23}$$

Substituting equation (22) into equation (23), the guidance command can be finally revealed as

$$\dot{\gamma} = -\frac{1}{t_{go}}\left(n(n-1)\hat{\gamma}_d + (2n-1)\varepsilon\right) + \dot{\lambda} \tag{24}$$

which allows a continuous selection of *n*.

5 Impact Angle Control Under Look-angle Constraint

In this section, a method exerting constraint on the look angle is developed based on the guidance command given by equation (24). For the purpose, the time-to-go estimated by the range-to-go and its rate are investigated. Performing as the key point of the strategy, the time-to-go is given by

$$t_{go} = \frac{r}{V\cos\varepsilon} \tag{25}$$

Replacing t_{go} with equation (25) in equation (24) yields

$$\dot{\gamma} = -\frac{V\cos\varepsilon}{r}\left(n(n-1)(\gamma_d - \lambda) + (2n-1)\varepsilon\right) + \dot{\lambda} \tag{26}$$

It can be seen that if the look angle has started within $\mp\pi/2$, equation (26) would provide $\dot{\gamma} \to \dot{\lambda}$ and $\dot{\varepsilon} \to 0$ when $\varepsilon \to \mp\pi/2$ due to the cosine term in the time-to-go, leading to a natural saturation of the

guidance command thus the look angle which is consequently held within the certain range. Originated from this property, the modified time-to-go with a biased term on the look angle is proposed as

$$t_{go} = \begin{cases} \dfrac{r}{V\cos\left(\dfrac{\pi}{2} - \varepsilon_{\max} + \varepsilon\right)}, & 0 \le \varepsilon < \varepsilon_{\max} \\ \dfrac{r}{V\cos\left(-\dfrac{\pi}{2} - \varepsilon_{\min} + \varepsilon\right)}, & \varepsilon_{\min} < \varepsilon < 0 \end{cases} \tag{27}$$

where $\varepsilon_{\min} < 0 < \varepsilon_{\max}$ represent the lower and upper limits of the look angle. Hence, when ε approaches its limits, equation (27) would increase to a very large value and eventually make the guidance command become $\dot{\lambda}$, causing the saturation as well as the constrained look angle. However, the modification will inevitably cause time-to-go error and negatively affects the guidance performance if the error remains till the very end of the engagement, so a switching logic is further given as

$$t_{go} = \begin{cases} \text{Eq. (27)}, & \text{sgn}(\dot{\varepsilon}) = \text{sgn}(\varepsilon) \\ \text{Eq. (25)}, & \text{sgn}(\dot{\varepsilon}) = -\text{sgn}(\varepsilon) \end{cases} \tag{28}$$

where $\dot{\varepsilon}$ is calculated from equation (14). Therefore, using equation (28) as the time-to-go is able to fulfill the look-angle constraint for the proposed impact angle control guidance methodology.

6 Simulation Results

In this section, the performance of the proposed impact angle control guidance law is illustrated through two simulated examples in which a missile is required to hit a stationary target 5 km downrange. Idealized flight condition is assumed firstly to demonstrate the ability of the proposed guidance law, followed by a subsection considering gravitational force, autopilot lag and constrained look angle to show the effectiveness in real applications. Wherever applicable, MATLAB® function *bvp4c* is employed to obtain the optimal solution subject to the desired impact angle while minimizing the total control effort, i.e. $\int a^2 \mathrm{d}t$.

6.1 Idealized Simulations

The simulated scenarios performed in this subsection assumes that the missile travels with a constant velocity of 200 m/s and maneuvers with idealized dynamics. The missile is deemed to hit the target when r<1 m and that is where the simulation terminates. Equation (25) is employed to determine the time-to-go required by the guidance law.

The results of the first set of simulations are depicted in Figure 2, where two subcases with different initial conditions, clarified in Table 2, are given to show the impact posed by the order of the polynomial. The flight path angle profile shown in Figure 2b indicates that the desired impact angles given in the first column of Table 2 are fulfilled, and the collision is ensured as the look-angle profile shown in Figure 2c is nullified at the end of the engagement. It is also observed that in Figs. 2a and 2d, increasing n allocates more maneuver to the early stage of the engagement, resulting in less demand of the terminal acceleration. As can be seen in Figure 2d, n = 3 leads to a well constrained terminal acceleration since $\dot{\varepsilon}(t_f) = 0$ is satisfied by the shaped polynomial. However, the total control effort

favors a lower *n*. Particularly when *n* = 2, the control efforts required by the proposed guidance law is only 4% larger than the optimal results as can be observed from Table 2.

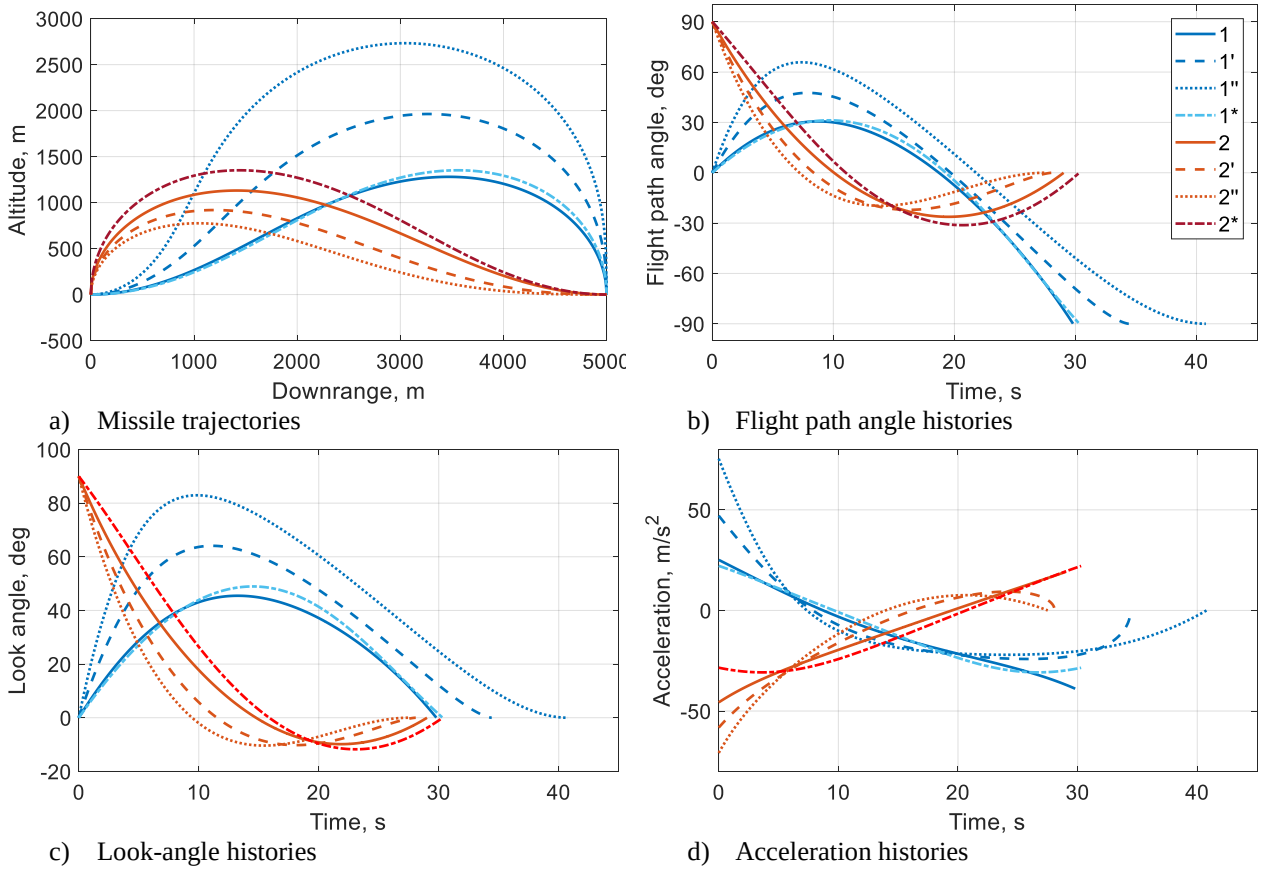

a) Missile trajectories b) Flight path angle histories

c) Look-angle histories d) Acceleration histories

Fig. 2 Simulation results under various values of *n*

Table 2 Total control effort ($\int a^2 \mathrm{d}t$, $\mathrm{m}^2/\mathrm{s}^3$)

	k: n = 2	k′: n = 2.5	k″: n = 3	k*: Optimal
1: $\varepsilon_i = 0°$, $\gamma_d = -90°$	1.25×10^4	1.48×10^4	2.08×10^4	1.23×10^4
2: $\varepsilon_i = 90°$, $\gamma_d = 0°$	1.27×10^4	1.43×10^4	1.64×10^4	1.22×10^4

6.2 Simulations under Autopilot Lag, Gravity and Look-Angle Constraint

In this subsection, a more realistic scenario is simulated. The autopilot dynamics is described as the first order latency between the command and the response with a time constant τ, specified in the last column of Table 3. The gravitational force causing the velocity variation of the missile is constant with $9.81\ \mathrm{m/s^2}$ and it is compensated in the direction perpendicular to the velocity vector. Besides, the FOV is also considered up to 50 deg in the subcases labeled with "On" in Table 3, constrained by the method proposed in Section 5. The missile initially has a velocity of 250 m/s and look angle of $\varepsilon_i = 15\ \mathrm{deg}$, is designated to hit the target vertically, i.e., $\gamma_d = -90°$.

Figure 3 presents the simulation results, where the case numbers labeled are in accordance with Table 3, where 3rd and 4th pairs are with *n*=2 and the rest *n*=3. In Figure 3a, it can be seen that the trajectories shaped by $\tau = 0.4\ \mathrm{s}$ are slightly higher than those of $\tau = 0.2\ \mathrm{s}$. Due to a larger value of *n*, pair 5/5' poses the most curved trajectory and the impact is delayed, similar to the phenomenon observed in 6.1. The flight path angle profile given in Figure 3b indicates that even with large dynamic delay and constrained look angle, the desired impact angle is well achieved in all subcases with satisfactory impact angle precision shown in Table 3, so is the miss distance. When the look-angle histories depicted

in Figure 3c are analyzed, it is most apparently that pair 5/6 and 5′/6′ validate the effectiveness of the proposed look-angle constraint strategy. As seen, the look-angle profiles of 5/5′ go up over 80 deg while those of 6/6′ are well confined in the limit. Since the constraint strategy is gradually modifying the guidance command instead of pressing a hard switch cutting the command whenever the look angle hits the boarder, it results in a smooth approaching progress towards the limit, providing a natural non-chattering attribute against noise. However, it is also observed that although in pair 3/3′ the look-angle limit is not exceeded, the constrained pair 4/4′ still leads to affected movement, leading to less usage of the look angle as well as a lower trajectory. The acceleration histories given in Figure 3d show that the cases with n = 3 require nearly no terminal maneuver. In contrast, those with n = 2 left the maximum acceleration at the end of the engagement. Besides, when the look angle is constrained, the total control effort of n = 3 is even more optimal than n = 2 (e.g., pair 3/6 in Table 3), possessing both the terminal acceleration and the consumption advantages in the acceleration performance.

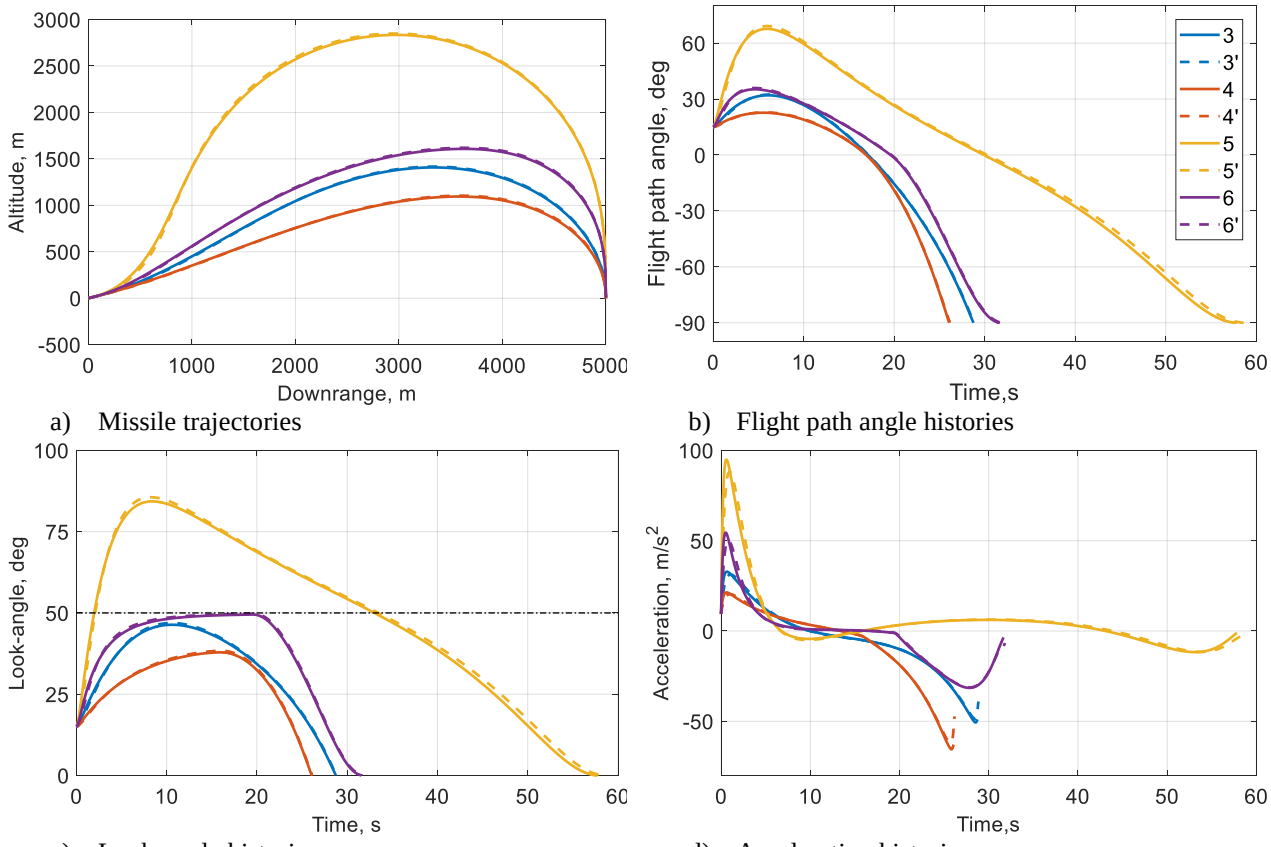

a) Missile trajectories b) Flight path angle histories

c) Look-angle histories d) Acceleration histories

Fig. 3 Simulation results under realistic condition

7 Conclusion

In this work, the impact angle control problem is investigated via shaping the look-angle profile with a generalized polynomial of time. After defining enough boundary conditions, the guidance gain is designed to fulfill the impact angle constraint. Linearized kinematics is employed to uncover the link between the desired impact angle and the guidance gain then the closed-form guidance law is derived for the nonlinear domain. In addition, a look-angle constraint strategy is proposed taking the advantage of the structure of the guidance law and the form of the time-to-go calculation. Simulation cases have fully demonstrated the effectiveness of the proposed guidance law for impact angle control under autopilot lag and gravity, as well as the proposed look-angle constraint method. The introduced approach might facilitate solutions for different trajectory shaping problems.

Table 3 Summary of the simulations under realistic condition

Scenario	Look-angle constraint	Impact angle error, deg	Miss distance, m	Control effort, m^2/s^3	τ, s
3	Off	0.0008	0.0918	1.07×10^4	0.2
3′		-0.0881	0.0816	1.06×10^4	0.4
4	On	-0.0044	0.2383	1.34×10^4	0.2
4′		-0.1974	0.0939	1.30×10^4	0.4
5	Off	0.0032	0.0825	1.77×10^4	0.2
5′		0.0123	0.0448	1.78×10^4	0.4
6	On	0.0158	0.0663	1.04×10^4	0.2
6′		0.1106	0.2016	1.03×10^4	0.4

References

[1] Kim, M., and Grider, K. V., “Terminal Guidance for Impact Attitude Angle Constrained Flight Trajectories,” IEEE Transactions on Aerospace and Electronic Systems, Vol. AES-9, No. 6, 1973, pp. 852–859.

[2] Erer, K. S., and Merttopcuoglu, O., “Indirect Impact-Angle-Control Against Stationary Targets Using Biased Pure Proportional Navigation”, Journal of Guidance, Control, and Dynamics, Vol. 35, No. 2, March-April 2012, pp. 700-704.

[3] Kim, T. H., Park, B. G., Tahk, M. J., "Bias-Shaping Method for Biased Proportional Navigation with Terminal-Angle Constraint", Journal of Guidance, Control, and Dynamics_, Vol. 36, No. 6, Nov.–Dec. 2013, pp. 1810-1816.

[4] Erer, K. S., Tekin, R., and Özgören, M. K., “Biased Proportional Navigation with Exponentially Decaying Error for Impact Angle Control and Path Following,” 24th Mediterranean Control and Automation Conference, IEEE, Athens, 2016.

[5] Ratnoo, A., and Ghose, D., “Impact Angle Constrained Interception of Stationary Targets”, Journal of Guidance, Control, and Dynamics, Vol. 31, No. 6, 2008, pp. 1817–1822.

[6] Ratnoo, A.,"Nonswitching Guidance Law for Trajectory Shaping Control," Journal of Guidance, Control, and Dynamics, Vol. 40, No. 10, 2017, pp. 724–732.

[7] Ryoo, C.-K., Cho, H., and Tahk, M.-J., “Time-to-Go Weighted Optimal Guidance with Impact Angle Constraints”, IEEE Transactions on Aerospace and Electronic Systems, Vol. 14, No. 3, 2006, pp. 483–492.

[8] Ratnoo, A., and Ghose, D., “State-Dependent Riccati-Equation-Based Guidance Law for Impact-Angle-Constrained Trajectories”, Journal of Guidance, Control, and Dynamics, Vol. 32, No. 1, January 2009, pp. 320-326.

[9] Kumar, S. R., Rao, S., and Ghose, D., "Sliding-Mode Guidance and Control for All-Aspect Interceptors with Terminal Angle Constraints," Journal of Guidance, Control, and Dynamics, Vol. 35, No. 4, 2012, pp. 1230–1246.

[10] Kumar, S. R., Rao, S., and Ghose, D., "Nonsingular Terminal Sliding Mode Guidance with Impact Angle Constraints," Journal of Guidance, Control, and Dynamics, Vol. 37, No. 4, 2014, pp. 1230–1246.

[11] Lee, C.-H., Kim, Tahk, M.-J., and Whang, I.-H., "Polynomial Guidance Laws Considering Terminal Impact Angle and Acceleration Constraints", IEEE Transactions on Aerospace and Electronic Systems, Vol. 49, No. 1, 2013, pp. 74–92.

[12] Dhabale, A., and Ghose, D., "Impact Angle Constraint Guidance Law Law using Cubic Splines for Intercepting Stationary Targets", AIAA Guidance, Navigation, and Control Conference, Minneapolis, Minnesota, August 2012.

[13] Zhou, Z., Yao, X., "Polynomial Guidance Law for Impact Angle Control with a Seeker Look Angle Limit", Proceedings of the Institution of Mechanical Engineers, Part G: Journal of Aerospace Engineering, Vol. 234, 2019, pp. 857-870.

[14] Erer, K. S., Tekin, R., and Özgören, M. K., "Look Angle Constrained Impact Angle Control Based on Proportional Navigation," AIAA Guidance, Navigation, and Control Conference, AIAA, Reston, VA, 2015, pp. 91–101.

[15] Hirwani, V., and Ratnoo, A., "Field-of-View Constrained Polynomial Guidance Law with Dual-Seeker Interceptors", AIAA Guidance, Navigation, and Control Conference, Kissimmee, Florida, January 2018, pp. 1325.

[16] Wang, X., Zhang, Y., Wu, H., "Sliding Mode Control Based Impact Angle Control Guidance Considering the Seeker′s Field-of-View Constraint," ISA Transactions, Vol. 61, 2016, pp. 49-59.

[17] Tekin, R., and Erer, K. S., "Switched-Gain Guidance for Impact Angle Control under Physical Constraints," Journal of Guidance, Control, and Dynamics, Vol. 38, No. 2, 2015, pp. 205–216.

[18] Tekin, R., A New Design Framework for Impact Time Control, PhD. Dissertation, Technical University of Munich, 2018.

[19] Ryoo, C. K., Cho, H., and Tahk, M. J., "Optimal Guidance Laws with Terminal Impact Angle Constraint," Journal of Guidance, Control, and Dynamics, Vol. 28, No. 4, 2005, pp. 724–732.